Guided resonance in Photonic Crystals

by

Pei Du

A thesis submitted in partial fulfillment of the requirements
for the degree of

Master of Science in Electrical and Computer Engineering

University of Wisconsin-Madison
May 2014

CERTIFICATE OF APPROVAL

This thesis is accepted and approved in partial fulfillment of the requirements for the Master of Science in Electrical and Computer Engineering.

Guided Resonance in Photonic Crystals

Pei Du

Date: 5/6/2014

Signed: ______________________

Zongfu Yu

Thesis Advisor

Abstract

The objective of this thesis research is to analyze the guided resonances in photonic crystal slabs. It introduces the different kinds of photonic crystals and focuses on photonic crystal slabs consisting of a square lattice of air holes. The guided resonances are created by the coupling between the guided modes above the light line and radiation modes. Specifically, we calculate the transmission spectra of the guided resonances.

Our work is mainly based on four parts. Firstly, we introduce the background of photonic crystals and then we discuss the properties of different kinds of photonic crystals. Next, we briefly discuss the software that we use to plot transmission spectra. Finally, we focus on band structure of guided resonances in photonic crystal slab, use time domain analysis including computational methods and line shape analysis by introducing a general and intuitive mode, and summarize the result.

The research in the thesis show the guided resonances are strongly confined in the dielectric slabs and coupled to radiation modes at the same time. Through the transmission spectra, we can see that it is modified from the result of uniform photonic slab. The new spectra contain some sharp resonant peaks and the line shape shows complex asymmetries which comes from the interference between direct and indirect pathways.

Keywords: Guided Resonances, Photonic Crystal Slabs, Transmission Spectra, Time Domain Analysis

ACKNOWLEDGEMENT

I would like to extend my sincerest gratitude to all those who supported and encouraged me during my graduate work at University of Wisconsin-Madison. I would first like to thank my advisor, Prof. Zongfu Yu, for his help, guidance and faith. Then, many thanks go to PHD students in Prof. Yu's group. They give me a lot of help on using software. Finally, I would like to express my gratitude to my family for their love, support and advice they have given to me throughout the years.

Table of contents

List of Figures

1. Introduction

Many of important breakthroughs in this century have resulted from a deeper understanding of the properties of materials. Our ancestors from the Stone Age through Ion Age have an increasing recognition of the utility of natural materials. Prehistoric people fashioned tools based on their knowledge of durability of stone and the hardness of iron. In each case, people learned how to find the useful properties of a material. With the development of the technology, people started to find the electrical properties of the material. Knowledge of semiconductor physics has allowed us to control the conducting properties of the material, thus initiating the transistor revolution in electronics. Then people realized that similar material may control the optical properties like changing the propagation of light, allowing light propagate in a certain direction or confined the light in a specific area, which is an analogy to semiconductor materials. This kind of optical material is called photonic crystal. A crystal is a periodic arrangement of atoms and modules. It is composed of periodic dielectric, metallo-dielectric or even nanostructures that affect the propagation of electromagnetic waves. A block of atoms and molecules is repeated in space, therefore leading to a periodic potential to an electron propagating through it, and the geometry of the crystal leads to many of conduction properties of the crystal.

Next, we will briefly introduce the history of photonic crystal. The term photonic crystal was first created in 1987 after Eli Yablonovitch and Sajeev John [1],[2] published two papers on photonic crystal. Before 1987, periodic multi-layer dielectric stacks such as Bragg reflectors can be regarded as the form of one-dimensional photonic crystal. Lord Rayleigh found that Bragg reflectors have one-dimensional photonic band gap and a spectral range of large reflectivity in 1987 [3]. Today, scientists and researchers put reflective coatings to improve the reflective coefficient of the mirror and they also put them into laser cavities such as VCSEL. Vladimir P. Bykov [4] first came out a detailed study of structure of one-dimensional photonic crystal and speculated what the same theory would be like if it is used in two-dimensional and three-dimensional photonic crystal. [5] The concept of three-dimensional photonic crystal was discussed by Ohtaka in 1979, [6] who also found the way to calculate the photonic crystal structure. However, their bright ideas were not known to people until Yablonovitch and John published their two papers, which focused on high dimensional periodic optical structures of photonic crystal. Yablonovitch's idea was to control the spontaneous emission of materials used by photonic crystal and John's motivation was to use photonic crystal to control light.

After that, research paper about photonic crystals began to increase. However, these papers only talked about the theoretical part of photonic crystal since it was hard to fabricate. In 1996, Thomas Krauss made first demonstration of two dimensional photonic crystals at optical wavelengths. [7] He provided the idea that people could borrow the idea from the semiconductor industry and use it in the photonic crystal. People then used techniques to make photonic crystal slab which can be used in integrated computer chips to enhance the optical processing of communication between chips. People also found that two-dimensional photonic crystal have commercial applications such as photonic crystal fibers which was first made by Philip Russell in 1998.

The development of three-dimensional photonic crystals process is slower because of the difficulty of its fabrication.

2. Construction of photonic crystal

2.1. One-dimensional photonic crystal

We begin discussion of photonic crystal with the simplest case, one dimensional photonic crystal. Even in this case, we can apply the electromagnetic theory and get the property of it like photonic band gaps and localized modes at defect.

The simplest photonic crystal is shown in Fig.1, they are alternating layers with different dielectric constants. This structure is widely used and it can be regarded as a perfect mirror with a frequency within a sharply defined band gap and localize their modes if there are any defects in the structure.

We first start to discuss the wave propagation in the one-dimensional photonic crystal. We can apply Maxwell's equations in this situation.

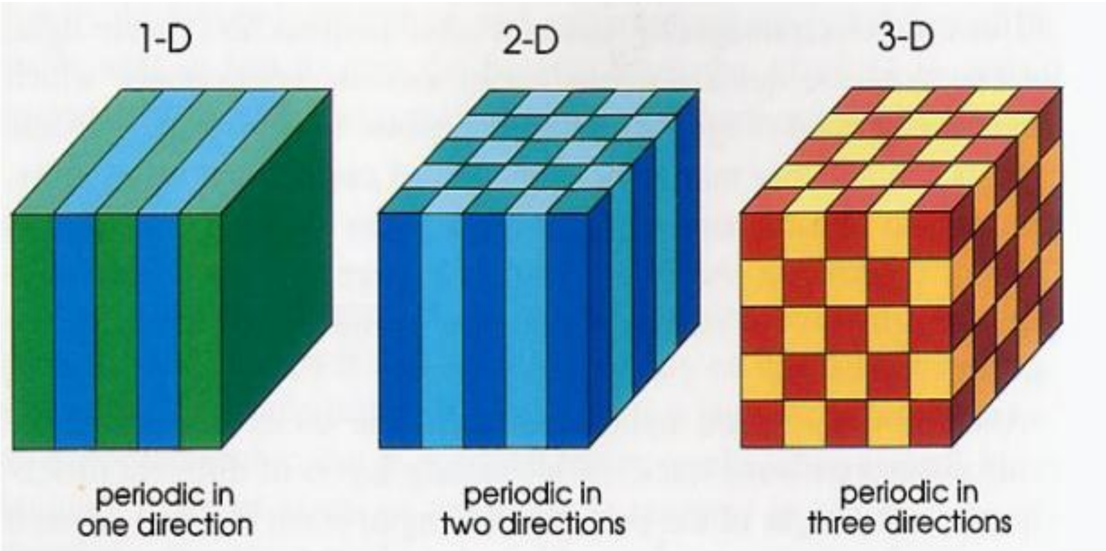

Figure 1. [8] Photonic crystal structure for 1-D, 2-D and 3-D situations

We can write the time-dependent Maxwell's equation in dielectric media as

$$\nabla \times H - \frac{\partial D}{\partial t} = 0 \quad (1)$$

$$\nabla \times E + \frac{\partial B}{\partial t} = 0 \quad (2)$$

If we assume the mode is in steady state, we can write the time harmonic mode as follows

$$H(r,t) = H(r)e^{iwt} \quad (3)$$

$$E(r,t) = E(r)e^{iwt} \quad (4)$$

Thus, Maxwell equations for this structure for the steady state become:

$$\nabla \times H(r) - iw \cdot \varepsilon(r)\varepsilon_0 E(r) = 0 \quad (5)$$

$$\nabla \times E(r) + iw \cdot \mu_0 H(r) = 0 \quad (6)$$

This equation can be expressed in magnetic field only:

$$\nabla \times \frac{1}{\varepsilon(r)} \nabla \times H(r) = \left(\frac{w}{c}\right)^2 H(r) \quad (7)$$

$\varepsilon(r), \mu(r)$ are the permittivity and permeability of the dielectric structure and c is the speed of light in dielectric structure.

Then we introduce the band structure of the photonic crystal. In figure 2, we show the photonic crystal band structures for on-axis propagation.

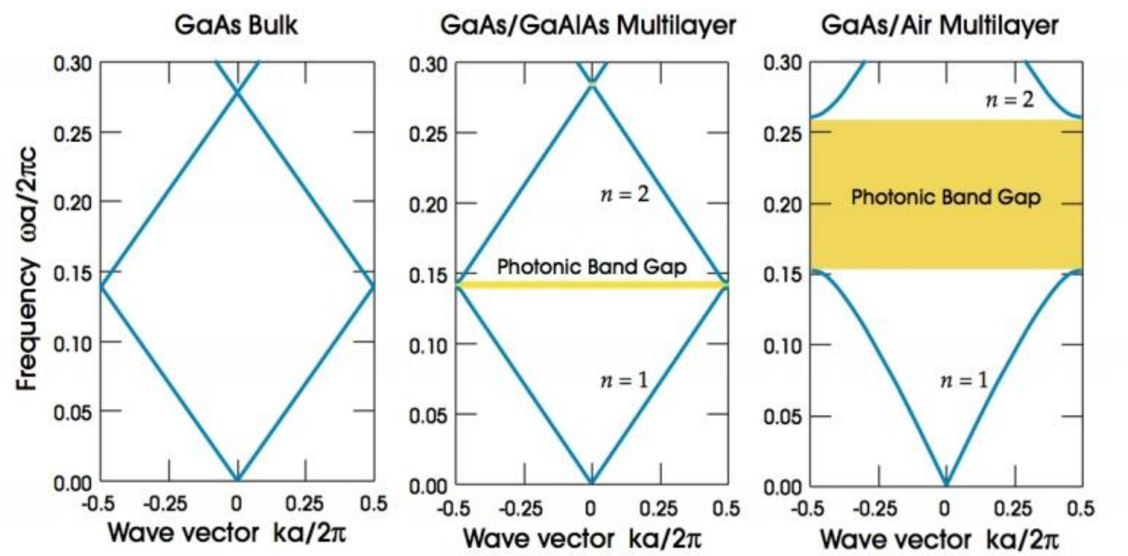

Figure 2. [8] Photonic crystal band structures shown for three different multilayer films, all of which have layers of width $0.5a$. Left: each layer has the same dielectric constant $\varepsilon = 13$. Middle: layers alternate between $\varepsilon = 12$ and $\varepsilon = 13$. Right: layers alternate between $\varepsilon = 13$ and $\varepsilon = 1$.

The left part of figure shows a uniform dielectric medium, so the band structure is very similar with that in the vacuum. The frequency spectrum is a light-line given by:

$$w(k) = \frac{ck}{\sqrt{\varepsilon}} \quad (8)$$

k is the propagation wave vector, c is the speed of light in the vacuum and w is the frequency of spectrum. Since we consider that k repeat itself outside the first Brillouin zone, the lines fold back into the zone when they reach the edges. The band structure of a nearly uniform medium in the middle part of the picture looks like the one that is in the left part. However, there is a significant difference between them. A gap appears between the upper branch and the lower branch of the lines. It's a frequency gap that means no modes exist in the crystal. As for the right part of the figure, the photonic band gap becomes wider since dielectric contrast becomes larger.

Then we will discuss the reflectivity of Bragg reflector when the wave is at normal direction, using transfer matrix method, we can draw a figure as follows:

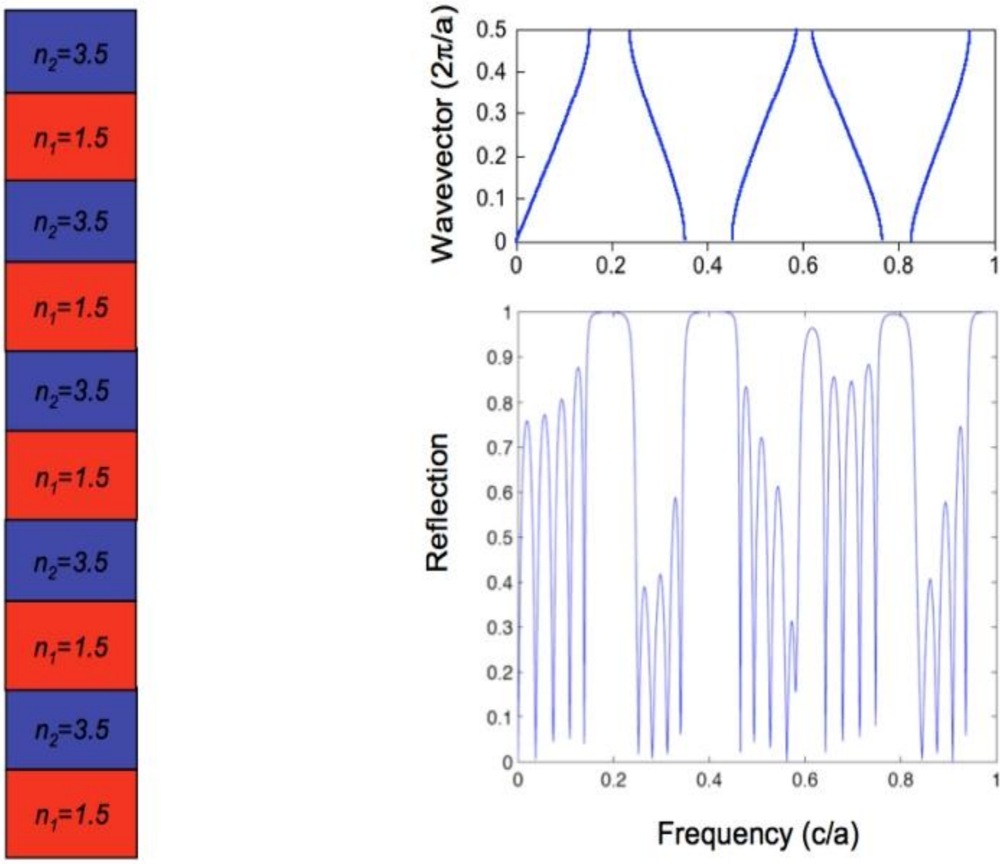

Figure 3. [8] Left: Medium with alternative dielectric constant; Above: dispersion relation of this structure; Below: The reflection coefficient with different frequency.

We can figure out that the reflection coefficient is 1 when it lies in a band gap. That means no propagation mode is allowed in a band gap of photonic crystal, which is very important.

Although it is true that no modes are allowed between the modes, when we send a light wave with frequency in the photonic band gap onto the face of the crystal from outside, the wave vector becomes complex. The wave amplitude decays exponentially into the crystal and the modes are evanescent and decay exponentially. We should emphasize that although evanescent modes are genuine solutions of the eigenvalue problem, they do not satisfy the translational-symmetry boundary condition of the crystal. It is not possible to excite them in a perfect crystal. Only a defect in an otherwise perfect crystal might sustain such a mode.

Now we will talk about the localized modes at defects. We have already known the features of a perfectly periodic system, so we can examine whether the system is broken by a defect or not, For instance, if a defect consists of a single layer of the one-dimensional photonic crystal that has a different width than the rest, the perfectly system is broken. But if we move many wavelengths away from the defect, the modes will behave as before.

2.2 Two-dimensional photonic crystal

The two-dimensional photonic crystal is a structure that is periodic along two of its axes and homogenous along the third axe, which is shown in the middle part of the Fig.1. $\overrightarrow{e_1}$ and $\overrightarrow{e_2}$ represent the real space lattice along lateral and vertical directions.

In order to delve into the band structure of two-dimensional photonic crystal, we should introduce the definition of the irreducible first Brillouin zone.

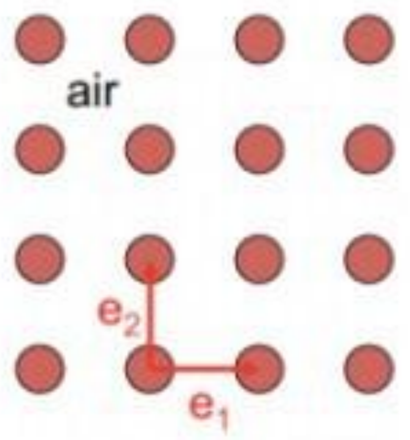

Figure 4. [8] Real space lattice vector of two-dimensional photonic crystal

As shown in the Fig.4 and Fig.5, we can express the real space lattice vector as:

$$e_1 = a(1,0) \tag{9}$$

$$e_2 = a(0,1) \tag{10}$$

And we can also express the reciprocal space lattice vector as follows:

$$g_1 = (1,0)2\pi/a \tag{11}$$

$$g_2 = (0,1)2\pi/a \tag{12}$$

So we define the irreducible first Brillouin zone of two dimensional photonic crystal as the shaded triangular area of the square. It is enclosed by three points Γ, X and M. We will discuss the band structure along the irreducible first Brillouin zone.

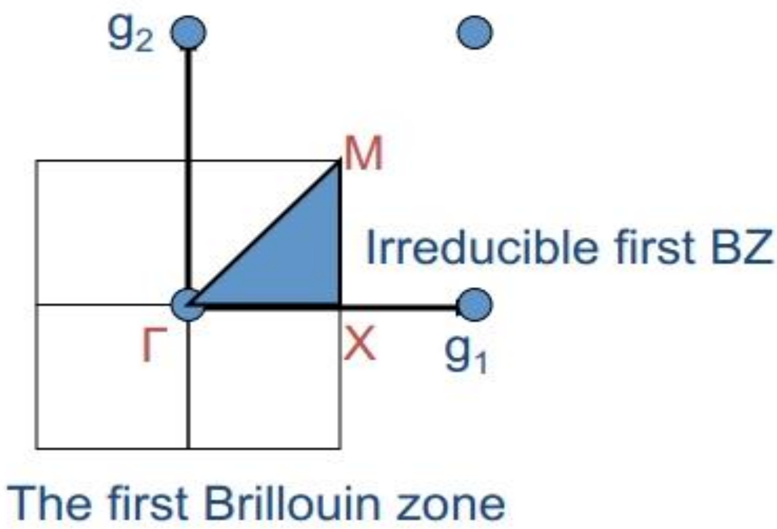

Figure 5. [8] The first Brillouin zone and irreducible first Brillouin zone of two-dimensional photonic crystal

In the following part, we will discuss two kinds two-dimensional photonic crystal. The first one is a square lattice of dielectric columns. We show the band structure of this case in Fig.6.

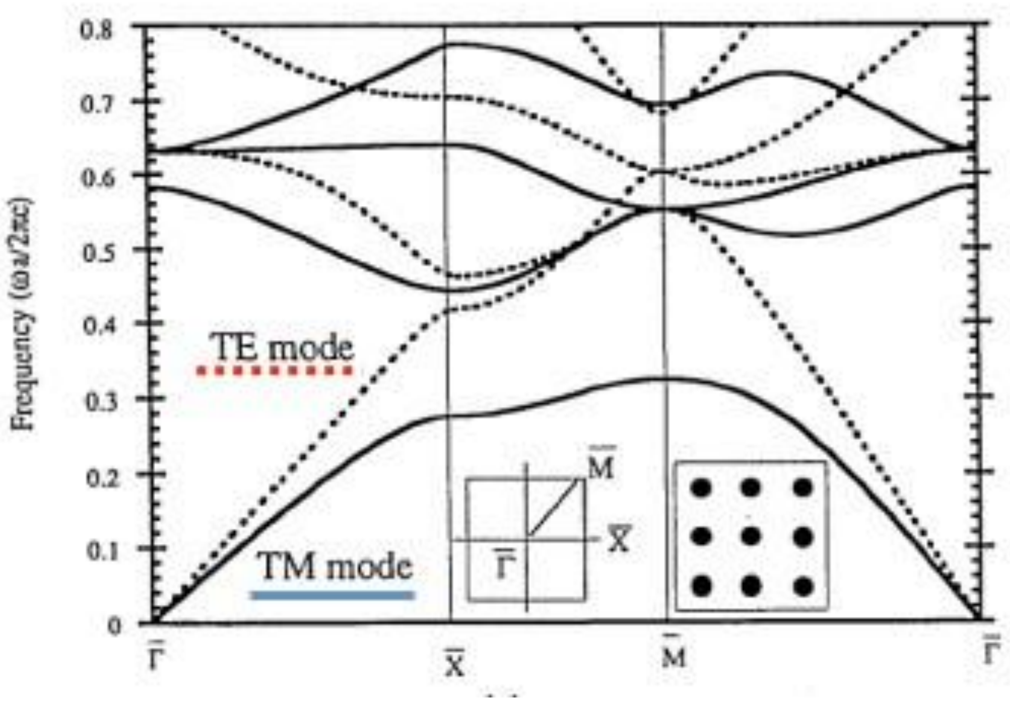

Figure 6. [9] The photonic band structure for a square array of dielectric columns with $r = 0.2a$. The solid lines represent TM modes and the dash lines present TE modes. The left inset shows the Brillouin zone, with the irreducible zone along point $\Gamma, \mathrm{X}, \mathrm{M}$. The right inset shows a cross-sectional view of the dielectric function, the circles with $\varepsilon = 8.9$ are embedded in air with $\varepsilon = 1$.

We call the first band and second band of TM modes "dielectric band" and "air band". And we can see for modes at Γ point, the fields are the same in each unit cell. And at X point, the fields are alternative in each unit cell along x direction. At M point, the pattern will be like a checkerboard, fields alternate in neighboring unit cells. However, for TE modes, things are different, which is shown in Fig.7.

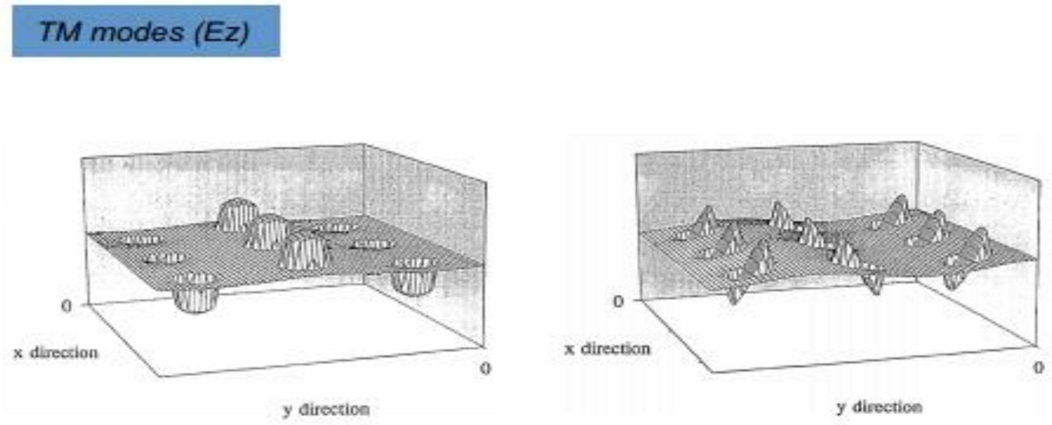

(a)

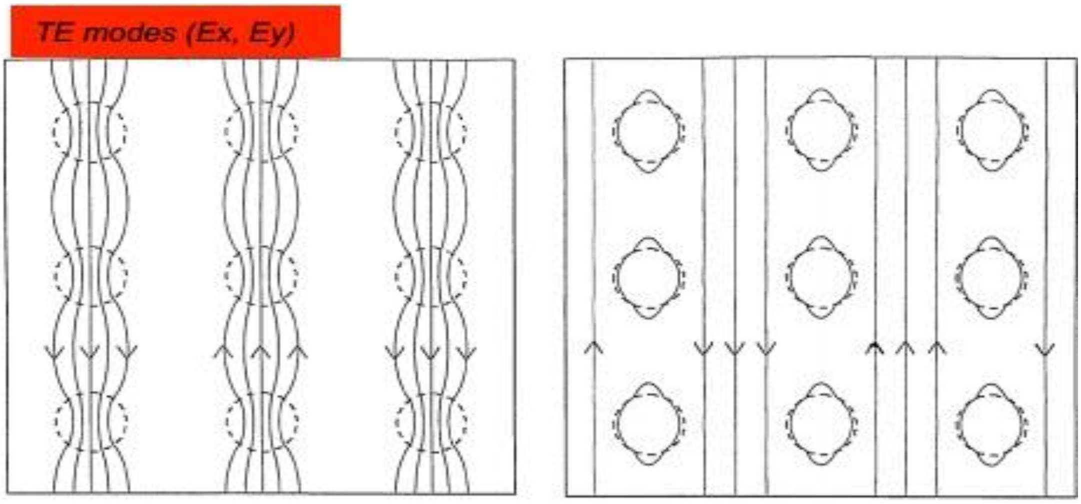

(b)

Figure 7. [9] Field pattern of first band and second band for (a) TM modes and (b) TE modes.

Another interesting phenomenon is that the band gap of TM mode is large and the band gap of TE mode is pretty small which means it favors TM gap. The reason is that the electric field is confined in the high dielectric region in the TM case. However, the electric field has to extend into the air region in the TE case. For the first band, most of its power is stored in the dielectric region and in contrast, most of power of the second hand is stored in the air region with a higher frequency than first band.

Let’s continue discussing a square lattice of dielectric veins. In contrary to the isolated structure, it favors TE gap instead of TM gap. We show the band structure of this lattice as shown in Fig.8.

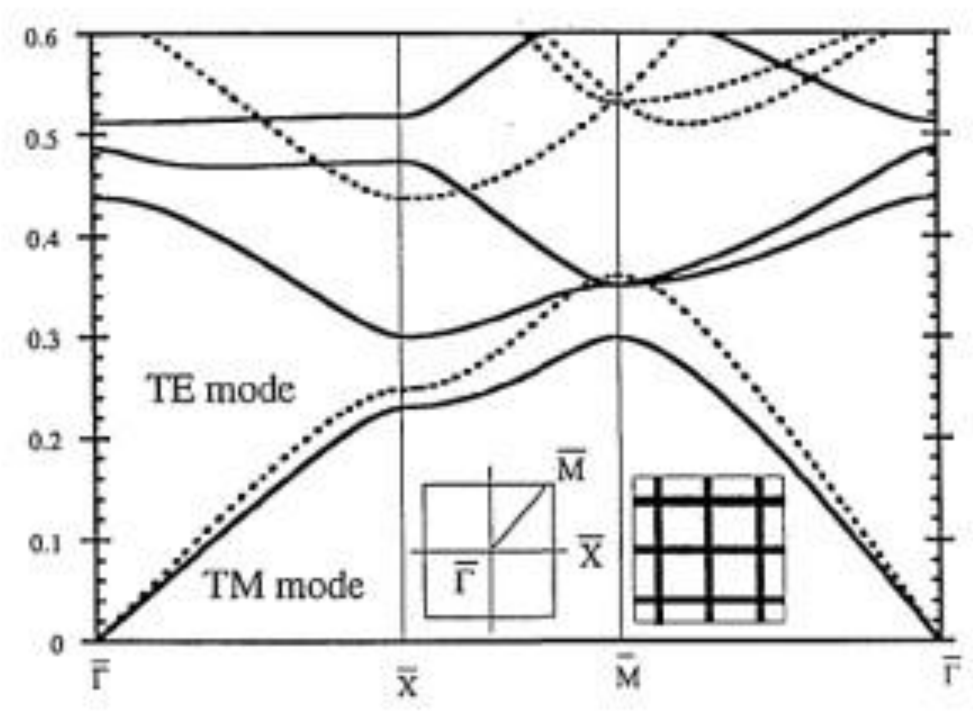

Figure 8. [9] The photonic band structure of a square array of dielectric veins with $\varepsilon = 8.9$. The solid line presents TM mode and the dash line presents TE mode. The left inset shows the Brillouin zone, with the irreducible zone along point $\Gamma, \mathrm{X}, \mathrm{M}$. The right inset shows a cross-sectional view of the dielectric function.

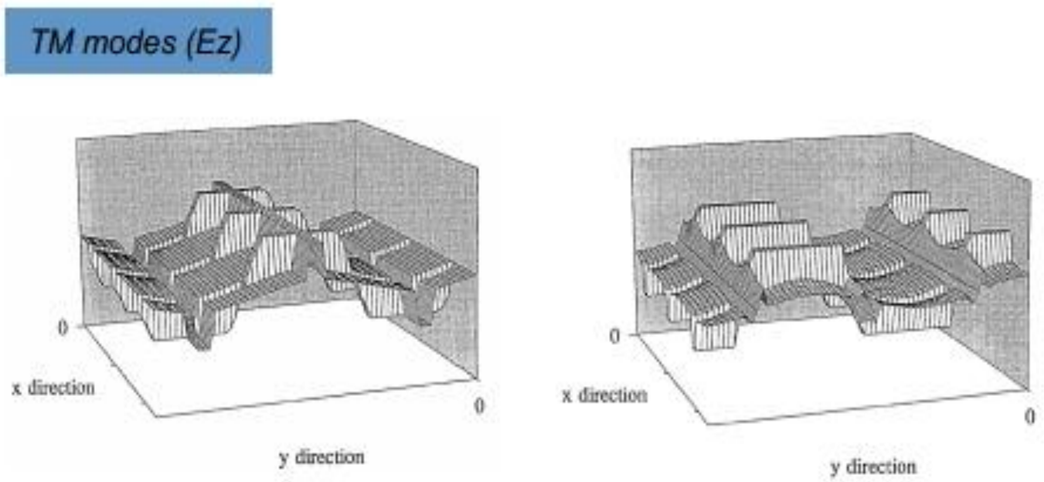

(a)

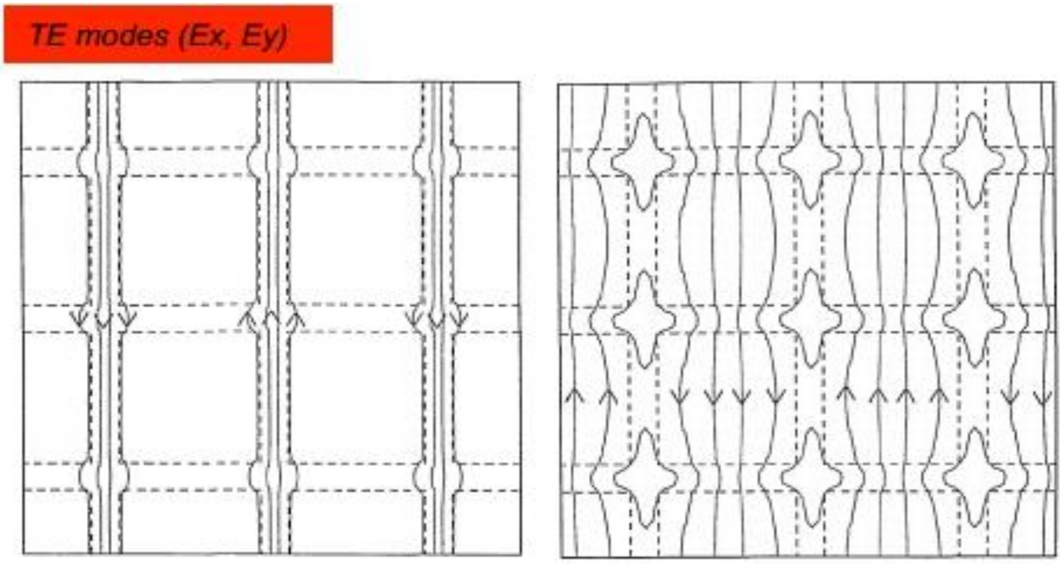

(b)

Figure 9. [9] Field pattern of first band and second band for (a) TM modes and (b)TE modes

We can see this lattice is complementary to the lattice of dielectric columns we talk about above. Usually, we call it a connected structure. It shows the opposite property of lattice of dielectric columns. For instance, we can see there is a gap for TE mode instead of TM mode from Fig.8, which is different from Fig.6.

Similarly, we also show the field patterns of the two modes. The fields are displayed for TM and TE mode in Fig.9.

2.3 Defect

2.3.1 Point Defect

Previously, we have discussed the band gap of two kinds of structures of two-dimensional photonic crystal. And we also find that no wave is permitted to propagate through the band gap. In order to make wave propagate through the band gap, we can remove a column or replace it with another column with different size to cause asymmetry. For instance, if we remove a rod from the lattice, we will create a cavity which is surrounded by reflecting walls. If the cavity has a proper size to support a mode in the band gap, the light will transmit through it. Since defect is very useful in transmission of photonic crystal, we talk about two kinds of defects in the following part. The first is named air defect which means the replaced rod is much smaller than other rods in the lattice. And the other kind is named dielectric defect which means the replaced rod is much larger than other rods in the lattice. In addition, we also point out that the frequency of defect is influenced by the volume of defect. That is, the frequency will decrease if the volume becomes larger, the result will be shown in Fig.10.

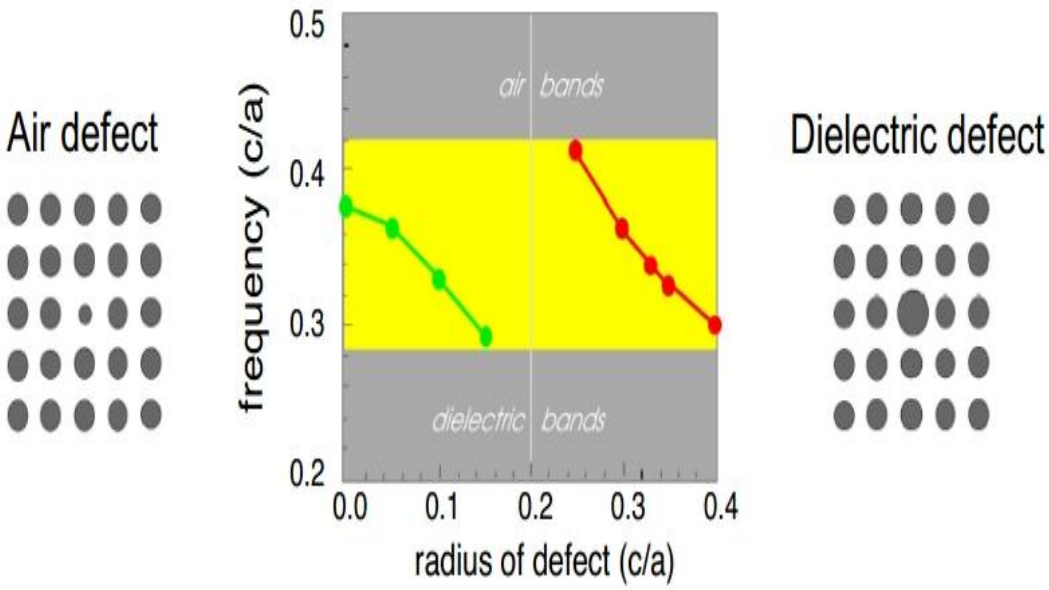

Figure 10. [8] The demonstration of air defect and dielectric defect is shown in the left and right part of the figure. In the middle of the figure, the green line represents that frequency varies with radius of defect in the air defect situation, the red line represents that frequency varies with radius of defect in the dielectric defect.

Historically, point defects in crystals were first considered in ionic crystals, not in the metal crystals. The reason is that some known properties of ionic crystals can be understood for the first time in terms of point defects, while on special properties of metals are in desperate need of an explanation.

2.3.1.1 Schottky Defect

There are also two typical kinds of point defects that are commonly used. The first is called Schottky defect.

A Schottky defect is a type of point defect in a crystal lattice. It is created by transferring an atom or ion from the original correct site to the surface of the sample. In ionic crystals, after the charged ions leave their lattice site, they will create vacancies. These vacancies are formed in stoichiometric units in order to maintain an overall neutral charge in the ionic solid. This type of defect is commonly seen in highly ionic compounds like NaCl.

The density of the solid crystal with defect is less than normal crystal because the total number of ions of a solid crystal with defect is less than that of a normal crystal.

Defects can modify the properties of a sample from that of a perfect crystal. For instance, when the frequency of incident light coincides with the frequency of defect as shown in Fig.10, the transmission will occur in the band gap. We can stimulate the transmission spectra and show them in Fig.11.

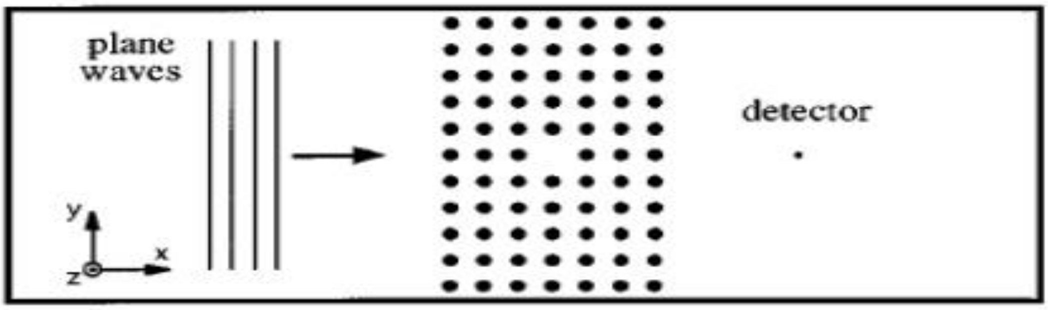

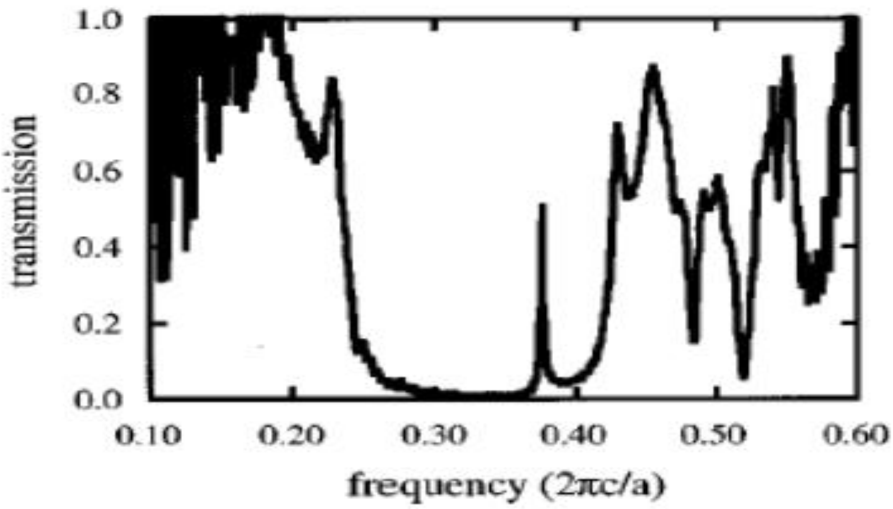

Figure 11. [10] The picture above shows the incident plane wave transmits through a lattice along *x* direction with a defect in the middle and a detector collects the transmission spectra. The picture below shows the transmission spectra of light, the light can transmit at the defect point.

2.3.1.2 Frenkel Defect

Frenkel defect is another type of point defect in a crystal lattice. If an atom leaves its place in the lattice site and is transferred to an interstitial position instead of surface, the defect is called Frenkel defect.

This effect does not appreciably change the density of the solid because it only transfers the ions within the crystal. It is commonly seen in ionic solids with large size difference between the anion and cation like ZnS.

2.3.2 Line Defect

So far, we have talked about point defect. Next, we will talk about line defect. Line defect usually comes from film growth process, dislocations in substrate continuing into film and contamination on substrate. In Fig.12, we show a simple case of line defect as well as the relationship between frequency and wave vector.

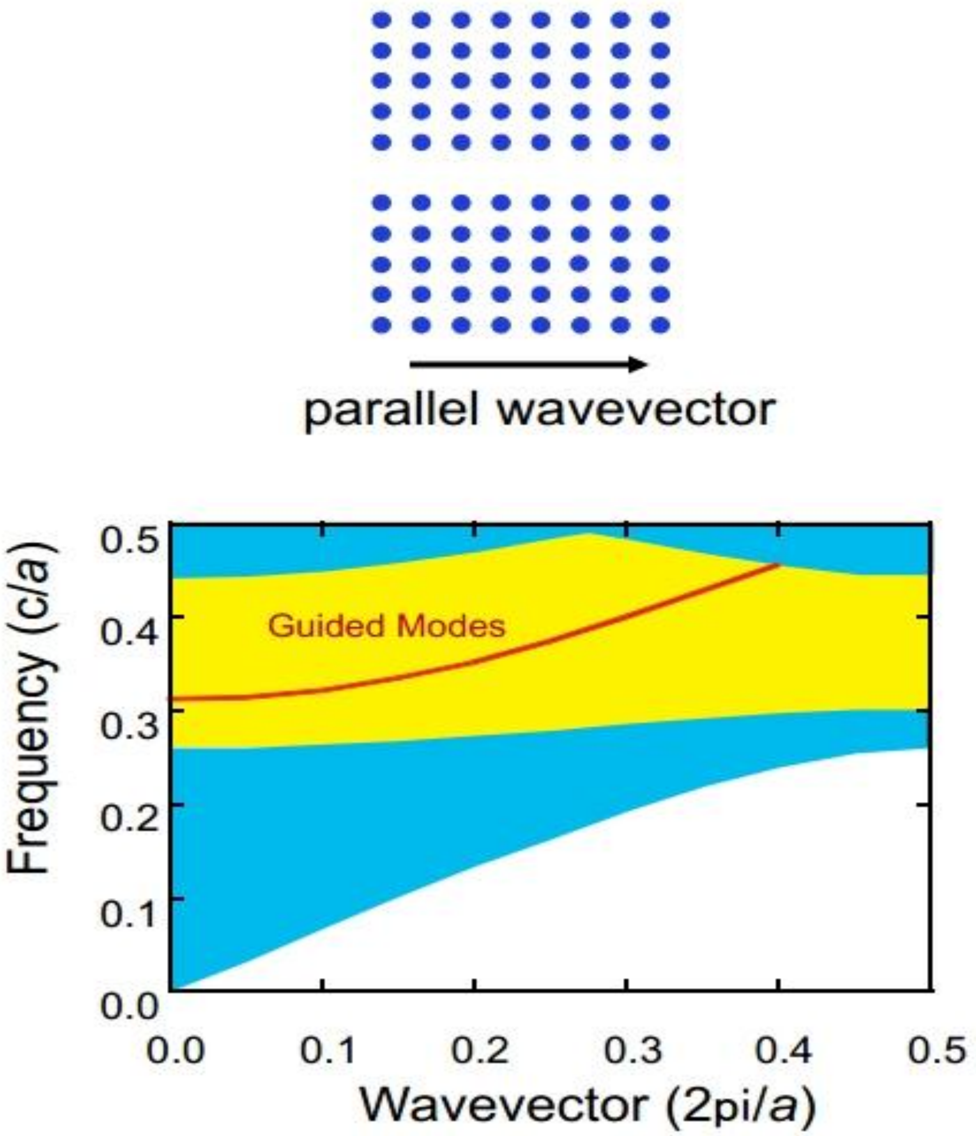

Figure 12. [8] Picture above is line defect and picture below is relationship between frequency and wave vector.

Basically, there are two kinds of dislocations, the screw dislocation and edge dislocation. The first type is hard to visualize and the second type is caused by the termination of a plane of atoms in the middle of the crystal. A mixture of both dislocations is common in crystals.

2.4 Comparison between photonic crystal and conventional waveguide

In this part, we will talk about the difference between photonic crystal and conventional waveguide. And we will find the advantages of photonic crystal waveguide compared to conventional waveguide.

The structure of photonic crystal waveguide and conventional waveguide is shown in Fig.13.

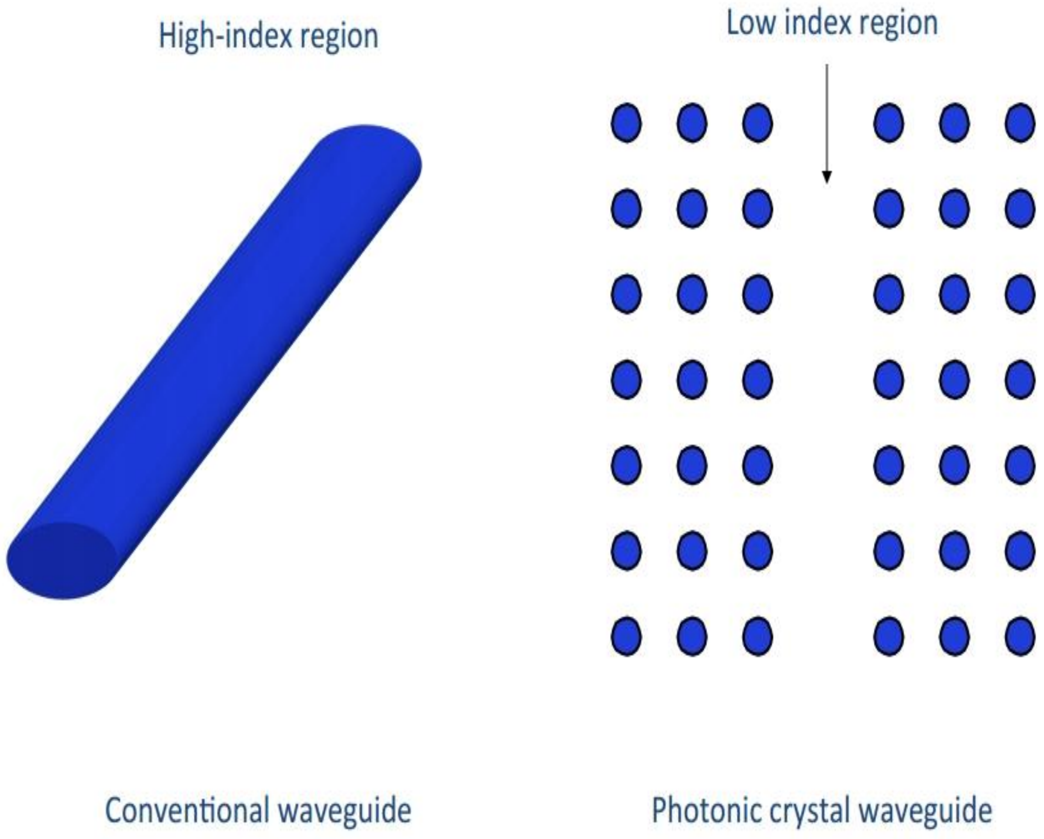

Figure 13. [8] The structure of conventional waveguide and photonic crystal waveguide. The blue dots represent the high index region.

Basically, there is no outstanding difference between two kinds of waveguides. However, when we apply for high transmission through sharp bends, the advantage of photonic crystal waveguide appears. For conventional waveguides, light will not transmit through the sharp bends smoothly. However, things are different in photonic crystal waveguide. From Fig.14, we show the electric field pattern for the case where the mode is completely confined in the guide and the light travels smoothly around the bend.

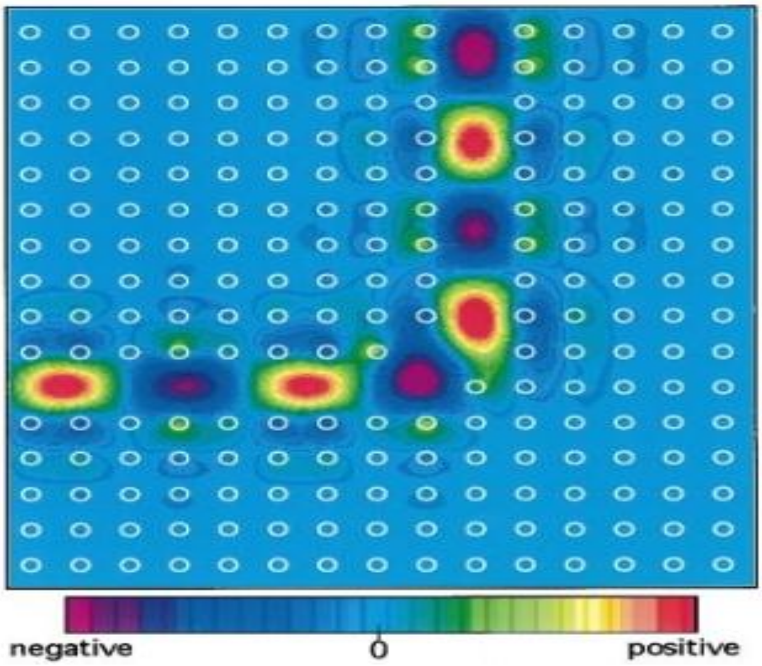

Figure 14. [11] Electric field pattern in the vicinity of the bend.

2.5 Three dimensional photonic crystal with complete band gap

There are a lot of possible geometries for a three-dimensional photonic crystal, but we are interested in those geometries that promote the existence of photonic band gaps. In two dimensional crystals, we talk about two kinds of construction of photonic crystals that are spots and veins. In three dimensional crystals, we may try creating crystal with dielectric tubes and spheres.

The first type is the crystal with dielectric spheres arranged in a diamond lattice. And the second type is also diamond lattice with cylindrical columns connecting lattice points. And the lattice points are joined to form a network of tubes.

Theoretically, complete photonic bands are rare in three dimensional photonic crystals because the gap must smother the entire Brillouin zone. Nevertheless, people still found several three dimensional photonic crystals yield sizable complete photonic band gaps.

Ho, Chan and Soukoulis were the first people to correctly predict that a complete band gap would exist in three dimensional photonic crystals. This crystal is the first type we discuss above. They found that complete band gap as long as the sphere radius is chosen appropriately.

Since three dimensional photonic crystals are not widely used, we just show the band structure for a diamond lattice which is shown in Fig.15.

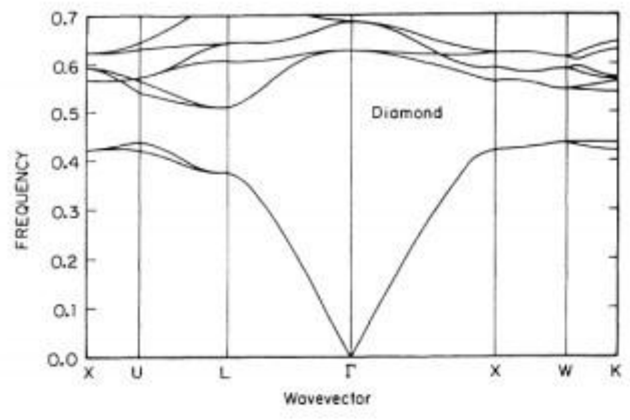

Figure 15. [8] The photonic band structure for a diamond lattice of air sphere in a high dielectric material.

3. Introduction of S^4

3.1 Introduction

S^4 (or simply S4) is the abbreviation of Stanford Stratified Structure Solver. It is based on a frequency domain code to solve the linear Maxwell's equations in layered periodic structures. The layered periodic structures which can be solved by S^4 is shown in Fig.16. Within the structure, it imposes Rigorous Coupled Wave Analysis (RCWA; also called the Fourier Modal Method (FMM)) and the S-matrix algorithm. And we use a Lua frontend, or alternatively, a Python extension to implement the process. S^4 was developed by Victor Liu of the Fan Group in the Stanford Electrical Engineering Department.[12]

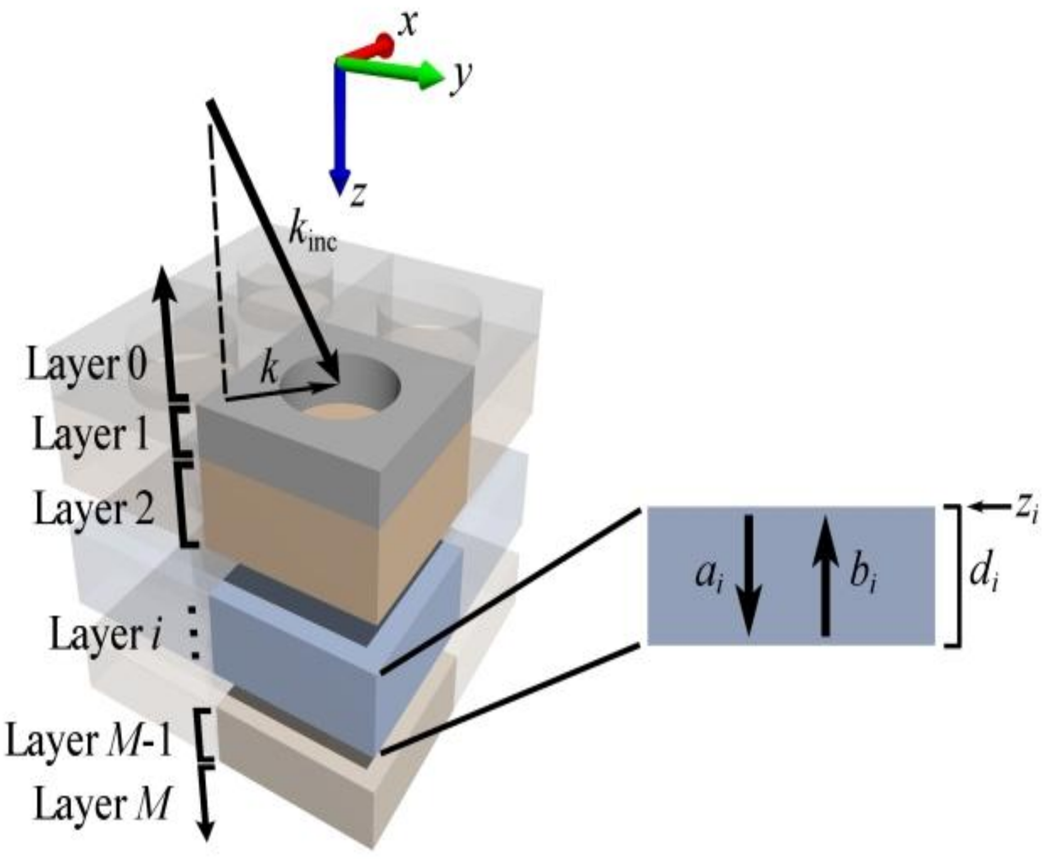

Figure 16. [12] Layered periodic structure solved by S^4

In addition, S^4 can compute reflection, transmission, or absorption spectra of structures consisted of patterned, planar and periodic layers. And we can get electromagnetic fields throughout the structure, as well as volume integrals and certain line. The spectra obtained from S^4 are extremely smooth, which allows us to make the local and global optimization easier to operate. [12]

3.2 Lua API reference

S^4 is built as a set of extensions to the Lua scripting language or Python language. Usage of S^4 involves writing a Lua script or Python script to call into various parts of S^4. [12]

S4 Library, specific functions and the code of this paper will be shown in Appendices.

4. Guided Resonances in photonic crystal slabs

4.1 Guided Resonances

Guided resonance[13]-[18] is a phenomenon which means the guided modes of an optical waveguide can be excited and simultaneously extracted by the introduction of a phase-matching element. Similar to guided modes, the electromagnetic power can be confined within the slab. However, the difference is that the guided resonances can transfer light from the slab to the external environment because they can couple with external radiation. Due to this property, a lot of applications can be made such as grating coupler, light-emitting diode [15],[19] and lasers.[20],[21]

4.2 Photonic Crystal Slab

Photonic crystal slab is very similar to two dimensional photonic crystals and it can be easily fabricated by existing techniques. It is a dielectric structure with two dimensional periodicity and confines light in the third direction by using index guiding. Photonic crystal slab has many properties from photonic crystal and simultaneously can be made with submicron length scales. The structure of photonic crystal slab is shown in Fig.17. These are two typical examples of photonic crystal slabs, a square lattice of dielectric rods in air and a triangular lattice of air holes in a dielectric slab. In this thesis, we will use the second structure with same index material to achieve transmission spectra.

4.2.1 *Q* factor

First, we introduce the definition of Q factor. Q factor is abbreviation of Quality factor. Q factor means the number of optical cycles (times 2π) before stored energy decays to $1/e$ of original value. Two ways are used to express the Q factor, definition of Q via energy storage and resonance bandwidth.

Assuming a time changing electric field proportional to $\cos(w_0 t)e^{-\frac{1\Gamma t}{2}}$, so the field is decaying and we use u to represent the energy density. The energy density decay will be proportional to $\Gamma e^{-\Gamma t}$. The figure is shown in Fig.17 to illustrate a time varying electric field with decaying tail.

Hence, the definition of Q factor via energy storage can be expressed as:

$$Q = 2\pi \frac{Stored\ Energy}{Energy\ Lost\ Per\ Optical\ Cycle} = 2\pi \frac{u(t)}{-\frac{du(t)}{dt}T} = \frac{2\pi}{\Gamma T} = \frac{w_0}{\Gamma} \quad (13)$$

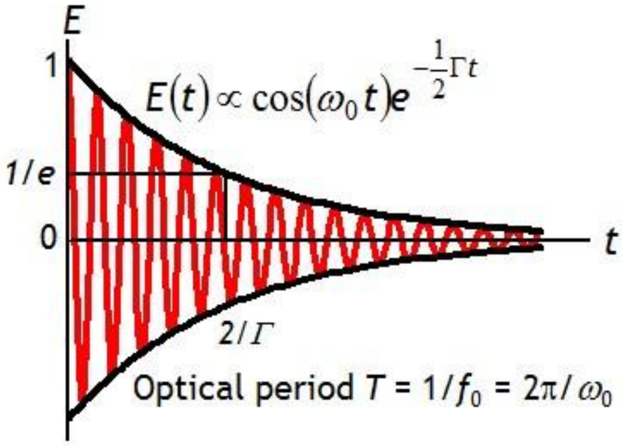

Figure 17. [22] A time varying electric field with decaying tail

When we apply Fourier transform to time domain, we can get the definition via resonance bandwidth. The intensity is proportional to $\frac{(\frac{\Gamma}{2})^2}{(w-w_0)^2+(\frac{\Gamma}{2})^2}$, which is the Lorentzian shape shown in Fig.18. Γ is equal to δw So the second definition can be expressed as

$$Q = \frac{w_0}{\delta w} = \frac{w_0}{\Gamma} \quad (14)$$

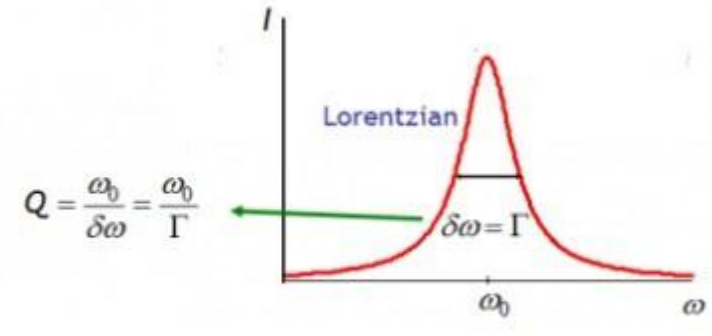

Figure 18. [22] Lorentzian shape

4.2.2 Light Line And Band Structure Of Photonic Crystal Slab

Next, we will talk about the concept of light line before we talk about band structure of photonic crystal slab.

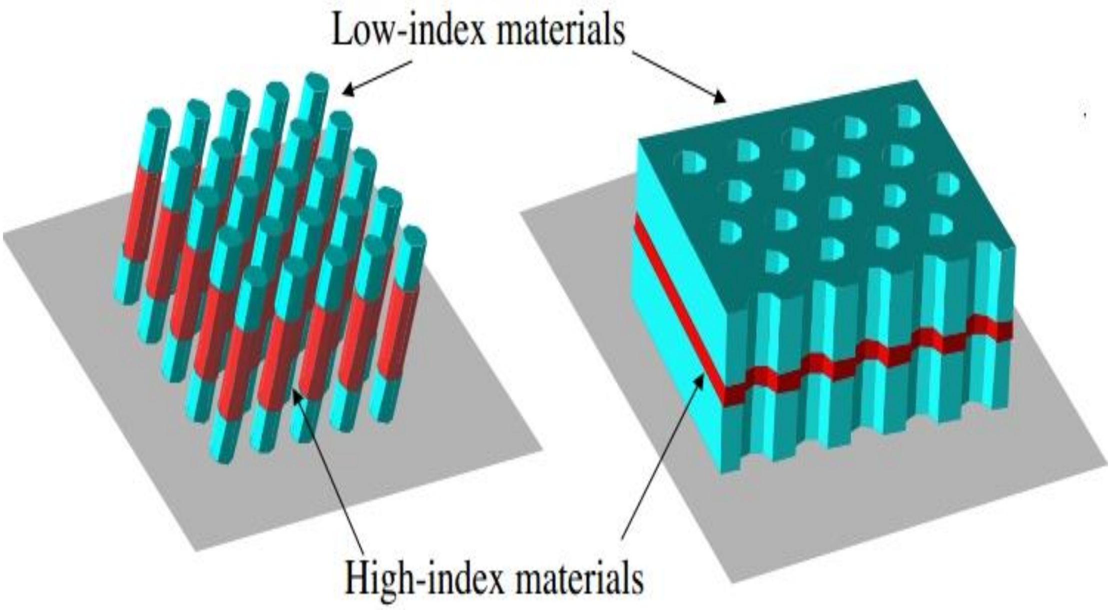

Figure 19. [8] The two structures of photonic crystal slab, the green part means low-index materials and the red part means high-index material. The left structure is square lattice of rods in air, the right structure is triangular lattice of holes in a dielectric slab.

First, we consider a uniform slab. Its light line is a straight line which is mentioned in equation (8). So we can plot the light line in the Fig.20 below and we also label radiation mode and guided mode in the figure.

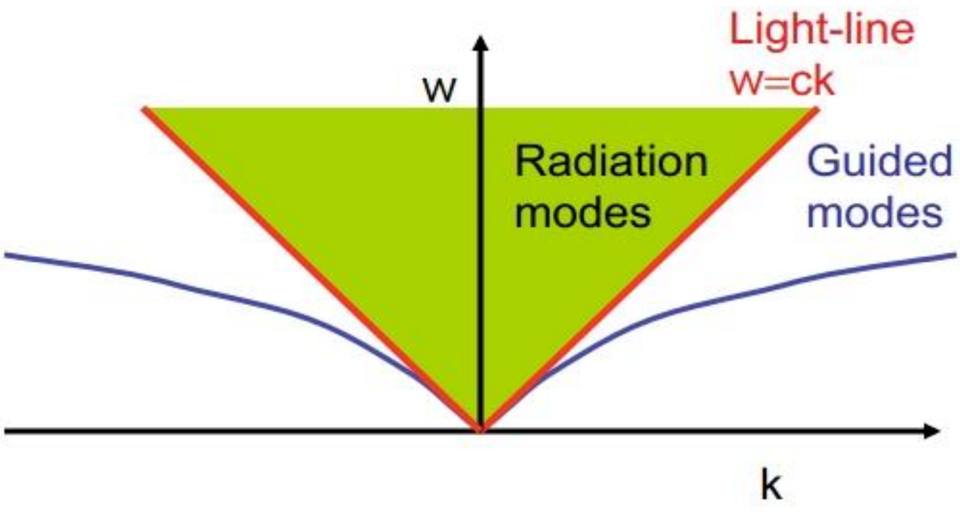

Figure 20. [8] Red line represents Light-line, Green area represents radiation mode, blue line represents guided modes.

Things are different when we focus on photonic crystal slab. An outstanding feature is that guided modes will couple within radiation region and they are called guided resonances as introduced in 4.1. The reason why they are called “guided” is that they are closely associated with guided modes in a uniform dielectric slab. However, the band structures are different between them. The band structure with even modes and odd modes of these two circumstances is shown in Fig.21 separately.

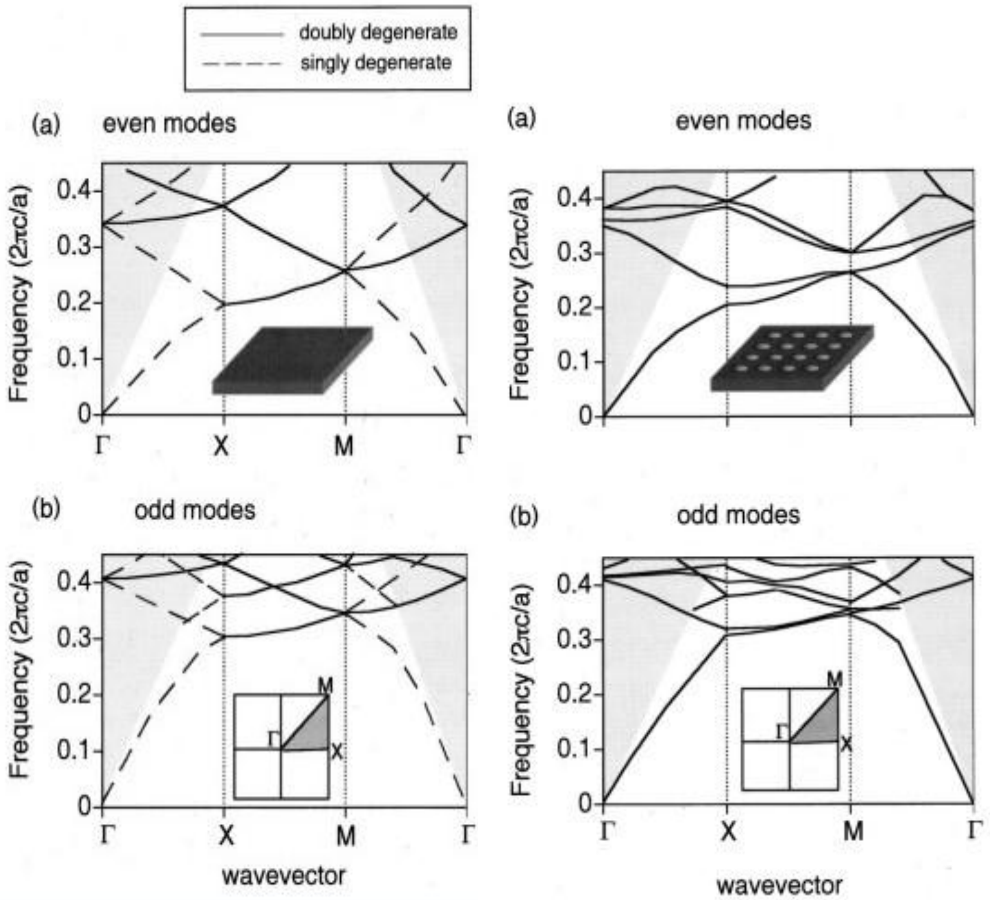

Figure 21. [16] The left part of the figure is the band structure for uniform dielectric slab, the band structure is plotted in a reduced-zone area with the square lattice constant *a*. The gray area represents radiation region and the lines represent guided modes. The right part of the figure is the band structure for photonic crystal slab with a square lattice of air holes introduced into a high-index dielectric slab. Solid lines within the radiation region represent the guided resonances of the slab.

From the figure above, we can see that the presence of air holes on the photonic crystal slab lower the degeneracy of the bands. That means for most k point expect Γ, X, M point, the bands become single degenerate. And at Γ point, the bands become double degenerate. Hence we can see the fourfold degeneracy at Γ point for uniform dielectric slab splits due to the existence of air holes.

4.3 Time Domain Analysis Of The Guided Resonances

In this section, we introduce the computational method that we use to solve transmission spectra. The computational domain is shown in Figure 20.

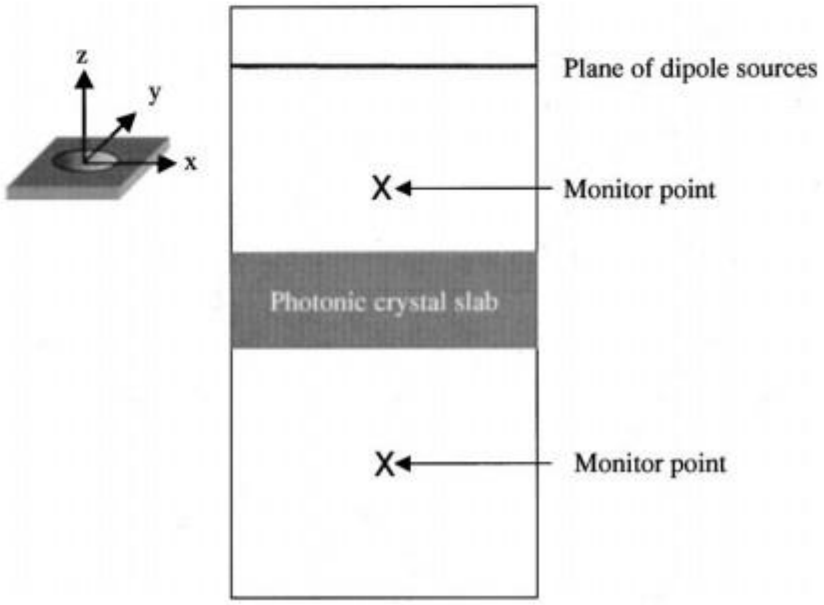

Figure 22. [16] Left part is a unit cell of the crystal with coordinate system. Right part is the cross section of the unit cell.

From Fig.22, we can see the computational domain encloses a unit cell of the photonic crystal. Thus, we can apply the boundary condition to the electric field E which is shown below on the four perpendicular facets of the slab.

$$\mathrm{E}(\vec{r}+\vec{a}) = e^{i(\vec{k}\cdot\vec{a})}E(\vec{r}) \tag{15}$$

$\vec{a}$ is the lattice vector of the square lattice, and $\vec{k}$ is the wave vector that is parallel to the photonic crystal slab. In addition, we apply Perfectly Match Layer (PML) absorbing boundary conditions to the top and bottom surface of the slab. When we place a plane of dipole sources near the top surface of the computational domain, the transmitted and reflected amplitudes are determined by the monitor points placed on the two sides of the slab. The two oscillating dipoles are separated by a distance vector $\vec{r}$, and the relative phase between them is $e^{i\vec{k}\cdot\vec{r}}$. The aim of placing two oscillating dipoles is to generate an incident plane with parallel wave vector $\vec{k}$. Hence, this computational method will allow us to calculate the response functions of the slab with different frequencies. When we apply first Fourier transforming the recorded time sequence of field amplitudes to the corresponding monitor points, we will get the transmission spectra.

Then we take a sample of photonic crystal slab consisting of a square lattice of air holes. The diameter of the hole is 200 nm and the thickness of the slab is 1 micrometer. In addition, we set the period of the holes as 500 nm and take the range of the wavelength from 600 nm to 1000 nm. Using the procedures of S^4 method and computational method which is set up above, we can plot the relationship between the transmission coefficient and the wavelength which is the spectra of the transmission. The code with notations of the procedure is shown in appendices. The transmission spectra of the sample is shown in Fig.23

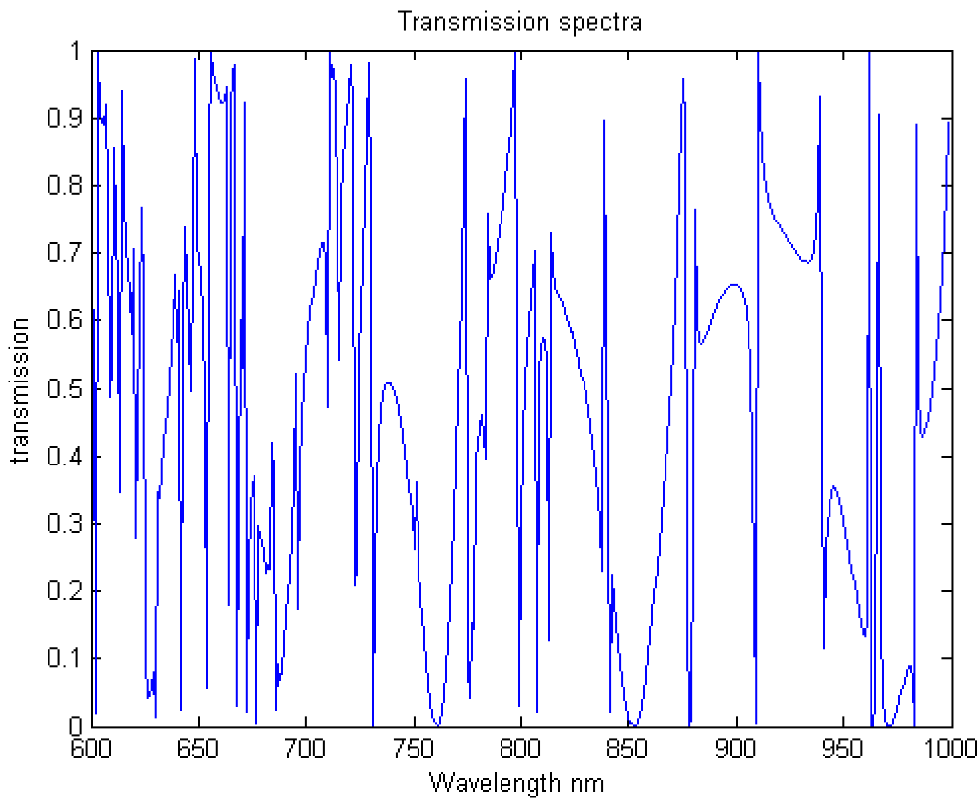

Figure 23. Transmission spectra of the sample

From the figure above, we can clearly see some sharp resonant features which are obtained from the guided resonances of the slab. The line shapes of the resonances are usually complex and asymmetric. A lot of researches have been done on guided resonances in structures with one dimensional periodicity.[21],[23]-[29] As for two dimensional periodic structure, we can solve guided resonances numerically by using vector coupled mode theory,[17] and rigorous coupled wave analysis method.[30] In this thesis, we will develop a new method from a time domain perspective. And we will observe the features of resonances when they become time domain, and we also provide a model to illustrate its physical meaning.

The transmission spectra are associated with time-varying electric field. Thus, we have to observe the features of the time dependence of the fields. The amplitudes of the electric field at the monitor points will have two stages if the transmission spectra are shown like Fig.21, an initial pulse and a long decay.

These two stages mean two pathways exist in the process of transmission. The initial pulse indicates a direct transmission process which means part of energy goes directly into the slab. The tail of long decay indicates indirect transmission process where guided resonances are excited by the remaining part of the energy. The power in the guided resonances decays slowly out of the crystal slab and form a long tail.

If we apply Fourier transforming, we will obtain the symmetric Lorentzian line shape, which can help us determine the quality factor Q of the resonance.

The interference between the two different pathways can determine the transmission property. We can also observe the similar phenomena in other fields such as solid-state physics and atom physics. This phenomenon is called Fano resonances. [31] In surface plasmons, we can also observe this interference phenomenon in metallic thin films.[32]

Now, we will consider the interference between the two pathways. Here, we take the quantitative method to explain the line shape. First, we show the expression of the transmitted amplitude and reflected amplitude as follows [16]:

$$\mathrm{t} = t_1 + a\frac{\gamma}{j(w - w_0) + \gamma} \tag{16}$$

$$\mathrm{r} = r_1 \pm a\frac{\gamma}{j(w - w_0) + \gamma} \tag{17}$$

where t, r are transmitted amplitude and reflected amplitude, a is the complex amplitude of the resonant mode. $t_1, r_1$are the direct transmission and reflection coefficients. w_0 is the center frequency of the resonance, and γ is the width of the Lorentzian from the resonance.

We can also see in Eq. (17), the sign becomes plus and minus. The reason is that we should use plus and minus to represent the even and odd mode of the resonance. The Lorentzian function in Eq. (16) and Eq. (17) refers to the decaying amplitudes of the resonances to the reflection side and transmission side of the slab. The decaying amplitudes to the two sides of the slab are in phase for an even mode, and the decaying amplitudes are 180 degree out of phase for an odd mode.

We know that the energy conversation,

$$|r|^2 + |t|^2 = 1 \tag{18}$$

In addition, we can also express t_1, r_1 as follows:

$$|r_1|^2 + |t_1|^2 = 1 \tag{19}$$

Combine Eqns. (18) and (19), we can determine the factor a. Plugging Eqns. (16), (17) and (19) into Eq. (18), we can get the following expression [16]:

$$-2|a|^2 \frac{\gamma^2}{(w-w_0)^2+\gamma^2} = 2|a||t_1 \pm r_1| \frac{\gamma}{\sqrt{(w-w_0)^2+\gamma^2}} \times \cos[\arg(a) - \arg(t_1 \pm r_1) - \arccos\left(\frac{\gamma}{\sqrt{(w-w_0)^2+\gamma^2}}\right) \tag{20}$$

If the condition is satisfied [16],

$$a = -(t_1 \pm r_1) \tag{21}$$

Now we will determine t_1 and r_1 [16],

$$t_1 = \frac{1}{\cos(k_{z1}d) - j\frac{k_{z0}^2 + k_{z1}^2}{2k_{z0}k_{z1}}\sin(k_{z1}d)} \tag{22}$$

$$r_1 = \frac{j\frac{k_{z0}^2 - k_{z1}^2}{2k_{z0}k_{z1}}\sin(k_{z1}d)}{\cos(k_{z1}d) - j\frac{k_{z0}^2 + k_{z1}^2}{2k_{z0}k_{z1}}\sin(k_{z1}d)} \tag{23}$$

k_x represents the parallel wave vector of the plane wave, ε_0 represents the dielectric constant of the vacuum, and ε_1 represents the dielectric constant of the slab with a thickness of d. k_{z0} *and* k_{z1} represents the wave vector parallel to *z* direction in the uniform slab and they are expressed as follows [16]:

$$k_{z0} = \sqrt{\varepsilon_0 \frac{w^2}{c^2} - k_x^2} \tag{24}$$

$$k_{z1} = \sqrt{\varepsilon_1 \frac{w^2}{c^2} - k_x^2} \tag{25}$$

For Eqns. (22) and (23), we take the positive frequency to make them consistent with Lorentzian functions in Eqns. (16) and (17).

Now, if we take $t_1 = 1$ and $r_1 = 0$, then the transmission and reflection coefficient becomes [16]:

$$t = \frac{j(w-w_0)}{j(w-w_0)+\gamma} \tag{26}$$

and

$$r = \mp \frac{\gamma}{j(w-w_0)+\gamma} \tag{27}$$

Thus the line shape becomes symmetric. In the general case when $r_1 \neq 0$, the line shape becomes asymmetric. The example is shown Fig.24.

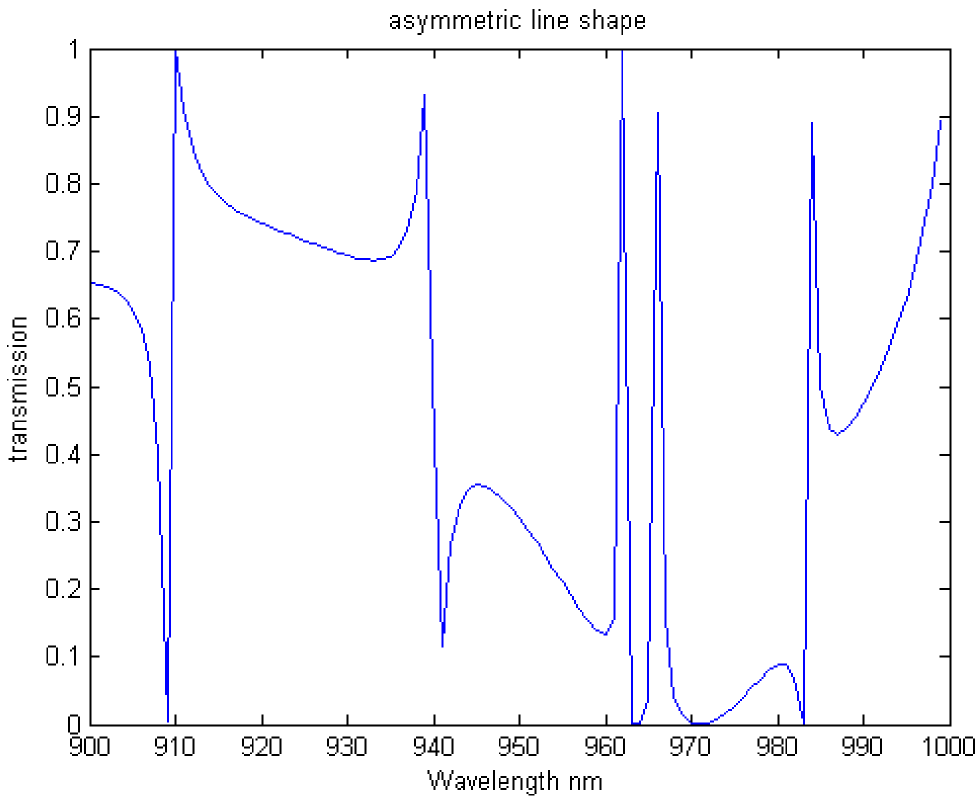

Figure 24. Example of asymmetric line shape

5. Conclusions and Future Work

In summary, we show the guided resonances in photonic crystal slabs by a three-dimensional frequency and an analytical model. The guided resonances are coupling between guided modes and radiation modes, which is strongly confined in the photonic crystal slab. Using software, we plot the transmission spectra of a photonic crystal slab consisting of a square of air holes with a diameter of 200 nm and a periodicity of 500 nm. Compared to the transmission spectra of a uniform photonic crystal slab, the spectra have been modified. We can observe the guided resonance modes with sharp peaks from the spectra. In addition, the line shape shows complex asymmetric characteristics. Hence, we use a general and intuitive physical model to explain the reason. In this model, we separate the field amplitude at the monitor point into two stages, the initial pulse and a long decaying tail. And the transmission property is determined by the interference between the direct and indirect pathways.

In the future research, we can use change the figure of the air holes such as rectangular holes to observe the phenomenon. And we can also change the diameter of the holes to calculate the transmission spectra to see the radius dependence of the resonance.

6. References

1. E. Yablonovitch (1987), "Inhibited Spontaneous Emission in Solid-State Physics and Electronics" (PDF), Physical Review Letters 58 (20): 2059–2062,

2. S. John (1987), "Strong localization of photons in certain disordered dielectric superlattices" (PDF),Physical Review Letters 58 (23): 2486–2489,

3. J. W. S. Rayleigh (1888), "On the remarkable phenomenon of crystalline reflexion described by Prof. Stokes"(PDF), Phil. Mag 26: 256–265

4. V. P. Bykov (1972), "Spontaneous Emission in a Periodic Structure", Soviet Journal of Experimental and Theoretical Physics 35: 269–273,

5. V. P. Bykov (1975), "Spontaneous emission from a medium with a band spectrum", Quantum Electronics 4 (7): 861–871

6. K. Ohtaka (1979), "Energy band of photons and low-energy photon diffraction", Physical Review B 19 (10): 5057–5067

7. T. F. Krauss, R. M. DeLaRue, S. Brand; Rue; Brand (1996), "Two-dimensional photonic-bandgap structures operating at near-infrared wavelengths", Nature 383(6602): 699–702

8. Photonic Crystals: molding the flow of light, John D. Joannopoulos, Robert D. Meade, Joshua N. Winn

9. R.D. Meade et al, Journal of Optical Society of America B, 10.330(1993)

10. P. R. Villeneuve, S. Fan, and J. D. Joannopoulos, "Microcavities in photonic crystals: mode symmetry, tunability and coupling efficiency," Phys. Rev. B 54, 7837 (1996).

11. High transmission through sharp bends in photonic crystal waveguides Attila Mekis, J.C.Chen, I. Kurland, Shanhui Fan, Pierre R. Villeneuve, and J.D. Joannopoulos, Physical Review Letters, Volume 77, Number 18

12. http://www.stanford.edu/group/fan/S4/

13. M. Kanskar, P. Paddon, V. Pacradouni, R. Morin, A. Busch, J. Young, S. Johnson, J. MacKenzie, and T. Tiedje, Observation of leaky slab modes in an air-bridged semiconductor waveguide with a two-dimensional photonic lattice, Appl. Phys. Lett. 70, 1438–1440 (1997).

14. Steven G. Johnson, Shanhui Fan, Pierre R. Villeneuve, and J. D. Joannopoulos, Guided modes in photonic crystal slabs, PHYSICAL REVIEW B VOLUME 60, NUMBER 8

15. M. Boroditsky, R. Vrijen, T. F. Krauss, R. Coccioli, R. Bhat, and E. Yablonovitch, “Spontaneous emission extraction and purcell enhancement from thin-film 2-d photonic crystals,” J. Lightwave Technol. 17, 2096–2112 (1999)

16. S. Fan and J. D. Joannopoulos, “Analysis of guided resonances in photonic crystal slabs,”

Phys. Rev. B 65, 235112 (2002).

17. P. Paddon and J. F. Young, “Two-dimensional vector-coupled-mode theory for textured planar waveguides,” Phys. Rev. B 61, 2090–2101 (2000).

18. V. Pacradouni, W. J. Mandeville, A. R. Cowan, P. Paddon, J. F. Young, and S. R. Johnson, “Photonic band structure of dielectric membranes periodically textured in two dimensions,” Phys. Rev. B 62, 4204–4207 (2000).

19. A. A. Erchak, D. J. Ripin, S. Fan, P. Rakich, G. S. Petrich, L. A. Kolodziejski, E. P. Ippen, and J. D. Joannopoulos,"Enhanced Coupling to Vertical Radiation Using a Two-Dimensional Photonic Crystal in a Semiconductor Light-Emitting Diode", Appl. Phys. Lett., 78(5): 563-565, (2001).

20. M. Meier, A. Mekis, A. Dodabalapur, A. Timko, R. E. Slusher, J. D. Joannopoulos, and O. Nalamasu Air-Hole Retained Growth by Molecular Beam Epitaxy for Fabricating GaAs-Based Photonic-Crystal Lasers Appl. Phys. Lett. 74 (1999) 7

21. S. S. Wang and R. Magnusson Theory and applications of guided-mode resonance filters Applied Optics, Vol. 32, Issue 14, pp. 2606-2613 (1993)

22.http://www.erbium.nl/nanophotonics/Nanophotonics%20Class%206%20-%20Microcavities.ppt

23. T. Ochiai and K. Sakoda Nearly free-photon approximation for two-dimensional photonic crystal slab. Phys. Rev. B 64, 045108 – Published 2 July 2001

24. S. S. Wang and R. Magnusso Design of waveguide-grating filters with symmetrical line shapes and low sidebands Optics Letters, Vol. 19, Issue 12, pp. 919-921 (1994)

25. A. Sharon, D. Rosenblatt, and A. A. Friesem Resonant grating–waveguide structures for visible and near-infrared radiation. JOSA A, Vol. 14, Issue 11, pp. 2985-2993 (1997)

26. T. Tamir and S. Zhang, "Resonant scattering by multilayered dielectric gratings," J. Opt. Soc. Am. A 14, 1607-1616, July 1997.

27. Scott M. Norton, G. Michael Morris, and Turan Erdogan Experimental investigation of resonant-grating filter lineshapes in comparison with theoretical models JOSA A, Vol. 15, Issue 2, pp. 464-472 (1998)

28. S. M. Norton, T. Erdogan, and G. M. Morris, “Coupled-mode theory of resonant-grating filters,” J. Opt. Soc. Am. A 14, 629–639 (1997).

29. Guy Levy-Yurista and Asher A. Friesem, Very narrow spectral filters with multilayered grating-waveguide structures Appl. Phys. Lett. 77, 1596 (2000)

30. S. Peng and G. M. Morris, “Resonant scattering from two-dimensional gratings,” J. Opt. Soc. Am. A 13, 993–1005 (1996).

31. U. Fano Effects of Configuration Interaction on Intensities and Phase Shifts

Phys. Rev. 124, 1866 – Published 15 December 1961

32. R. V. Andaloro, H. J. Simon, and R. T. Deck Temporal pulse reshaping with surface waves Applied Optics, Vol. 33, Issue 27, pp. 6340-6347 (1994)

APPENDIX

All top level functions of S4 are located in the S4 library. These functions mainly return objects which can be manipulated to obtain desired results.

S4 Library

(1)
S4.NewSimulation()
Returns a new blank Simulation object.

Usage:

S = S4.NewSimulation()
Arguments:

None.
Return values:

S
A new Simulation object.
(2)
S4.NewSpectrumSampler(f_start, f_end, options)
Returns a new SpectrumSampler object.

Usage:

sampler = S4.NewSpectrumSampler(f_start, f_end, options)
Arguments:

f_start, f_end
(number) Starting and ending frequencies of the frequency range in which to sample.
options
(table) A table of options controlling the sampling behavior. The keys and expected values are described below. If any option is not specified, the default value is used. Any out-of-range values are clamped to the valid range.
InitialNumPoints
(integer) The initial number of (uniformly spaced) sample points to use. If this value is not large enough, fine features may be missed. The default is 33.
RangeThreshold

(number) The threshold below which the difference between adjacent result values will not cause an interval to be subdivided. The default is 0.001.
MaxBend
(number) The cosine of the maximum bend angle of the normalized angle between adjacent segments. For angles larger than the maximum bend angle, one of the adjacent intervals is subdivided. The default bend angle is 10 degrees.
MinimumSpacing
(number) The relative frequency space (relative to the sampling interval size) below which subdivision will not occur. The default is 1e-6.
Parallelize
(boolean) Allows multiple frequency points to be solved in parallel. This option affects which methods can be called for a SpectrumSampler object. The default is false.
Return values:

sampler
A new SpectrumSampler object.
(3)
S4.NewInterpolator(type, table)
Returns a new Interpolator object.

Usage:

```
interpolator = S4.NewInterpolator('type', {
    {x1, {y1_1, y1_2, ... }},
    {x2, {y2_1, y2_2, ... }},
    ...
})
```

Arguments:

type
(string) Type of interpolation to use.

'linear'
Performs linear interpolation (and extrapolation) between values.
'cubic hermite spline'
Uses a cubic Hermite spline interpolation with Kochanek-Bartels tangents (really just a Catmull-Rom spline).
table
The second argument should be a table of tables. Each subtable should have as its first element the abscissa of a data sample, and the second element should be a table of all the ordinate values. The ordinate ordering is clearly important, and only the number of ordinate values for the first abscissa value determines the assumed number of ordinate values for the remaining abscissae.
Return values:

interpolator
A new Interpolator object.
(4)
S4.SolveInParallel(layername, ...)
Forces the computation of a layer solution for several simulation objects in parallel. When compiled without thread support, the computations are done serially.

Usage:

S4.SolveInParallel('layer', Sa, Sb, ...)
Arguments:

layer
(string) The name of the layer for which solutions should be computed. If the simulation objects do not have layer matching the provided name, then no solve is performed for that object.
Sa, Sb, ...
(Simulation object) The set of Simulation objects for which solutions are computed. It is useful to use the Clone() method to make copies.
Return values:

None.
(5)
S4.ConvertUnits(value, from_units, to_units)
Performs unit conversions.

Usage:

S4.ConvertUnits(value, from_units, to_units)
Arguments:

value=
(number) The value to convert.
from_units, to_units
(string) The units in which value is currently expressed, and the desired units. Currently supported units:

Lengths: “um”, “nm”, “m”, “cm”, “mm” Energies: “eV”, “J” Frequencies: “THz”, “GHz”, “Hz”, “rad/s”
Return values:

The converted value, or nil if no conversion was possible.
(6)
S4.Integrate(func, range1, range2, ..., opts)
Performs adaptive numerical integration in an arbitrary number of dimensions.

Usage:

integral,error = S4.Integrate(func, range1, range2, ..., opts)
Arguments:

func
(function) The function to integrate. It should take a number of arguments matching the number of range parameters passed in (the number of independent variables), and return a single number.
range1, range2, ...
(table) Each table should contain two elements corresponding to lower and upper limits of integration for the corresponding variable.
opts
(table) Options to the integration routine. This table is distinguished from an integration limit range by the presence of string keys. The options are:

MaxEval
(integer) Default is 1000000. Places an upper limit on the number of function evaluations allowed.
AbsoluteError
(number) Default is 0. Sets the termination criterion for the absolute error in the integral.
RelativeError
(number) Default is 1e-6. Sets the termination criterion for the relative error in the integral.
Parallelize
(boolean) Default is false. If true, the integrand may be evaluated in parallel. In this case, the function must accept an integer as the first argument corresponding to the number of evaluations required, and subsequent parameters are tables containing the set of independent variables for each evaluation. The function should then return a table containg all the results in the same order.
Return values:

Returns the integrated value and an estimate of the error.

Parameter Specification

(1)
Simulation:SetLattice(L)
Simulation:SetLattice({x1, y1}, {x2, y2})
Sets the real-space lattice vectors.

Usage:

S:SetLattice(L)
S:SetLattice({x1,y1}, {x2,y2})

Arguments:

This function can take a single numeric argument, which sets the period for a 1D lattice. This function can also take two table arguments, each of which must have two numeric elements. The first table specifies the x- and y-coordinates of the first lattice basis vector, while the second table specifies the second basis vector. The basis vectors should have positive orientation (the cross product of the first with the second should yield a vector with positive z-coordinate).

Return values:

None

(2)

Simulation:SetNumG(n)

Sets the maximum number of in-plane (x and y) Fourier expansion orders to use. All fields and eigenmodes of the system use the same Fourier basis of the same dimension.

The computation time is roughly proportional to the cube of this number, and the memory usage is roughly proportional to the square.

Usage:

S:SetNumG(n)

Arguments:

n

(integer) The desired maximum number of Fourier orders to use. This number is an upper bound because internally, the Fourier lattice k-vectors (referred to as the G-vectors) are found in a symmetry-preserving manner starting from the origin and retaining those of shortest length. To obtain the actual number of Fourier orders used, use GetNumG().

Return values:

None

(3)

Simulation:AddMaterial(name, {eps_r, eps_i})

Simulation:AddMaterial(name, eps_tensor)

Adds a new material with a specified dielectric constant.

Usage:

```
S:AddMaterial(name, {eps_r, eps_i})
S:AddMaterial(name, {
	{xx_r, xx_i}, {xy_r, xy_i}, {xz_r, xz_i},
	{yx_r, yx_i}, {yy_r, yy_i}, {yz_r, yz_i},
	{zx_r, zx_i}, {zy_r, zy_i}, {zz_r, zz_i}
	})
```

Arguments:

name

(string) The name of the material. Each material must have a unique name.

eps_r, eps_r

(number) The real and imaginary parts of the relative permittivity of the material. The imaginary part should be positive.

xx_r, xx_i, xy_r, ...

(number) Components of the relative permittivity tensor of the material. Currently the xz, yz, zx, and zy components are ignored and assumed to be zero.

Return values:

None

(4)

Simulation:SetMaterial(name, {eps_r, eps_i})

Simulation:SetMaterial(name, eps_tensor)

Updates an existing material with a new dielectric constant or adds a material if none exists.

Usage:

```
S:SetMaterial(name, {eps_r, eps_i})
S:SetMaterial(name, {
	{xx_r, xx_i}, {xy_r, xy_i}, {xz_r, xz_i},
	{yx_r, yx_i}, {yy_r, yy_i}, {yz_r, yz_i},
	{zx_r, zx_i}, {zy_r, zy_i}, {zz_r, zz_i}
	})
```

Arguments:

name

(string) The name of the material to update, or the name of a new material if no material by that name exists.

eps_r, eps_r

(number) The real and imaginary parts of the relative permittivity of the material. The imaginary part should be positive.

xx_r, xx_i, xy_r, ...

(number) Components of the relative permittivity tensor of the material. Currently the xz, yz, zx, and zy components are ignored and assumed to be zero.

Return values:

None

(5)

Simulation:AddLayer(name, thickness, material)

Adds a new unpatterned layer with a specified thickness and material.

Usage:

S:AddLayer(name, thickness, material)
Arguments:

name
(string) The name of the layer. Each layer must have a unique name.
thickness
(number) The thickness of the layer.
material
(string) The name of the material which comprises the layer. With patterning, this is the default (background) material of the layer.
Return values:

None
(6)
Simulation:SetLayer(name, thickness, material)
Updates an existing layer with a new thickness and removes all layer patterning. If no matching layer is found, adds a new unpatterned layer with a specified thickness and material. The behavior is undefined if the new material does not match the old material during an update (currently, the new material is ignored, but this may change in the future). If only the thickness needs to be modified, use SetLayerThickness().
Usage:

S:SetLayer(name, thickness, material)
Arguments:

name
(string) The name of the layer to update. If no layer by that name exists, a new layer is created with this name.
thickness
(number) The new thickness of the layer.
material
(string) The name of the material which comprises the layer.
Return values:

None
(7)
Simulation:SetLayerThickness(name, thickness)
Updates an existing layer with a new thickness. Previously cached layer eigenmodes are preserved, making this function the preferred way to update a layer's thickness.
Usage:

S:SetLayerThickness(name, thickness)

Arguments:

name
(string) The name of the layer to update.
thickness
(number) The new thickness of the layer.
Return values:

None
(8)
Simulation:AddLayerCopy(name, thickness, original_name)
Adds a new layer with a specified thickness, but identical patterning as another existing layer. Note that this merely creates a reference to the copied layer; further patterning of the copied layer also affects the new layer. Additionally, a copy of a copy cannot be made.
Usage:

S:AddLayerCopy(name, thickness, original_name)
Arguments:

name
(string) The name of the new layer, different from the layer being copied.
thickness
(number) The thickness of the new layer.
original_name
(string) The name of the layer which whose pattern is to be copied. That layer cannot itself be a copy of a layer.
Return values:

None
(9)
Simulation:SetLayerPatternCircle(layer, material, center, radius)
Adds a (filled) circle of a specified material to an existing non-copy layer. The circle should not intersect any other patterning shapes, but may contain or be contained within other shapes.
Usage:

S:SetLayerPatternCircle(layer, material, center, radius)
Arguments:

layer
(string) The name of the layer to pattern. This layer cannot be a copy of another layer.
material
(string) The name of the material which fills the interior of the circle.
center

(numeric table, length 2) x- and y-coordinates of the center of the circle relative to the center of the unit cell (the origin).
radius
(number) Radius of the circle.
Return values:

None
(10)
Simulation:SetExcitationPlanewave({phi, theta}, {s_amp, s_phase}, {p_amp, p_phase}, order)
Sets the excitation to be a planewave incident upon the front (first layer specified) of the structure. If both tilt angles are specified to be zero, then the planewave is normally incident with the electric field polarized along the x-axis for the p-polarization. The phase of each polarization is defined at the origin (z = 0).
Usage:

S:SetExcitationPlanewave({phi,theta}, {s_amp, s_phase}, {p_amp, p_phase}, order)
Arguments:

phi, theta
(number) Angles in degrees. phi and theta give the spherical coordinate angles of the planewave k-vector. For zero angles, the k-vector is assumed to be (0, 0, kz), while the electric field is assumed to be (E0, 0, 0), and the magnetic field is in (0, H0, 0). The angle phi specifies first the angle by which the E,H,k frame should be rotated (CW) about the y-axis, and the angle theta specifies next the angle by which the E,H,k frame should be rotated (CCW) about the z-axis. Note the different directions of rotations for each angle.
s_amp, p_amp
(number) The electric field amplitude of the s- and p-polarizations of the planewave.
s_phase, p_phase
(number) The phase of the s- and p-polarizations of the planewave, relative to z = 0 (the beginning of the first layer).
order
(number) An optional positive integer specifying which order (mode index) to excite. Defaults to 1. This is the same index that GetDiffractionOrder returns.
Return values:

None
(11)
Simulation:SetFrequency(freqr, freqi = 0)
Sets the operating frequency of the system (and excitation).
Usage:

S:SetFrequency(freqr, freqi)
Arguments:

freqr

(number) The (real) frequency of the excitation. This is not the angular frequency (the angular frequency is 2pi times of this).

freqi

(number) The imaginary frequency of the system. This parameter is typically not specified and assumed to be zero. When specified (typically for mode solving), this parameter should be negative for a physical (decaying in time) system.

Return values:

None

Coding of Transmission Spectra

```
--General Setup
S = S4.NewSimulation()


S:SetLattice({0.5,0}, {0,0.5})
--square lattice,200nm


S:SetNumG(90)

--Material Definition
S:AddMaterial("Si",{3.5^2,0})

S:AddMaterial("Vacuum",{1,0})

--Material Structure Definition
t_si = 1 -- thickness of silicon laye,1um

d_hole = 0.2 -- diameter


S:AddLayer('AirAbove',0,'Vacuum')
S:AddLayer('Top layer',t_si,'Si')
S:SetLayerPatternCircle('Top layer','Vacuum',{0,0},d_hole/2)

S:AddLayer('Bottom',0,'Vacuum')
```

```
--Incident Wave Definition
S:SetExcitationPlanewave(
	{0,0},	-- incidence angles (spherical coordinates: phi in [0,180], theta in [0,360])
	{0,0},	-- s-polarization amplitude and phase (in degrees)
	{1,0})	-- p-polarization amplitude and phase

--S:UsePolarizationDecomposition()


--Calculation of Spectrum
for lda = 0.6,1,0.001 do -- I use 0.901 instead of 0.9 to make sure that the loop will go up to 0.9. If you use 0.0002 step, you may need to use 0.9001.
	freq = 1/lda
	S:SetFrequency(freq)

	forward, backward = S:GetPoyntingFlux('AirAbove',0)
	lamda = lda*1000
	ref = -1*backward
	print(lamda,ref)
end
```